Anomalously enhanced lifetimes of low angular momentum Rydberg states in singly charged alkaline-earth metal ions

Simon Euchner,[1] Weibin Li,[2] and Igor Lesanovsky[1,2]

[1] *Institut für Theoretische Physik and Center for Integrated Quantum Science and Technology, Universität Tübingen, Auf der Morgenstelle 14, 72076 Tübingen, Germany*

[2] *School of Physics and Astronomy and Centre for the Mathematics and Theoretical Physics of Quantum Non-Equilibrium Systems, The University of Nottingham, Nottingham, NG7 2RD, United Kingdom*

arXiv:2609.24874v1 [physics.atom-ph] 21 Sep 2026

Trapped ions excited to high-lying electronic states, so-called Rydberg states, open new opportunities for quantum simulation and quantum computing. Generally, the fidelity of quantum coherent operations critically depends on the longevity of Rydberg states. However, scaling laws predict that the lifetimes of Rydberg states in singly charged alkaline-earth metal ions are 16 times shorter, compared to their neutral atom counterparts. Here, we show that this is not generally the case. We report an anomalous lifetime enhancement of certain low angular momentum ionic Rydberg series by factors larger than eight. The anomaly is present at both zero and finite temperature, although it is caused by different mechanisms. At zero temperature, the anomalously enhanced lifetimes are caused by accidental cancellations of the relevant dipole transition matrix elements, while at room temperature the anomaly originates from the enlarged energetic separation of ionic Rydberg levels with respect to neutral-atom levels.

Introduction. Neutral alkali-metal atoms excited to high-lying electronic states, so-called *Rydberg* states [1], constitute one of today's most advanced platforms for controlling single quantum mechanical degrees of freedom. The key ingredients responsible for the success of Rydberg atoms are their long lifetimes together with strong electronic state-dependent dipolar interactions [2–4]. Rydberg states can also be excited in trapped ion crystals [5–7]. Compared to arrays of neutral atoms, crystals of Rydberg ions may offer certain advantageous features: they provide strong, electronic-state-independent confinement [8, 9] for both low-lying states and Rydberg states and they offer collective vibrational modes which can be spatially delocalised over the whole ion crystal. This opens new opportunities for the quantum simulation of so-called *conical intersections* in molecular potential-energy surfaces [10–14], the study of excitation energy transport [15], the creation of electron-phonon entanglement [16], the exploration of electronic state-dependent molecular conformational changes [7], and the realisation of sub-microsecond entangling gates [17–19] for digital quantum computing. Moreover, the possibility to cool the ion crystal's vibrational degrees of freedom [20–22], in principle even in the Rydberg state, may open a route towards the study of long-time dissipative dynamics.

A potential downside of quantum simulation and computation with ionic Rydberg states is that their lifetimes are generally expected to be substantially shorter than those of Rydberg states in neutral atoms. This is seen as follows: the lifetimes of Rydberg states scale as $\tau \sim \mu_{\mathrm{i,f}}^{-2}\lambda_{\mathrm{i,f}}^{3}$ [23]. Here $\mu_{\mathrm{i,f}}^{2}$ is the radial transition dipole matrix element [24] between the initial Rydberg state $|i\rangle$ and the final state $|\mathrm{f}\rangle$, and $\lambda_{\mathrm{i,f}}$ is the wavelength of the photon emitted upon decay. Rydberg states in alkali-metal atoms and alkaline-earth metal ions closely resemble Rydberg states of Hydrogenic ions with effective nuclear charge $Z_{\mathrm{eff}} = 1$ and $Z_{\mathrm{eff}} = 2$, respectively. The analytical solution for the eigenstates of the Hydrogenic ion with nuclear charge Z_{eff} leads to the so-called *Hydrogenic* scaling laws $\mu_{\mathrm{i,f}} \sim Z_{\mathrm{eff}}^{-1}$ and $\lambda_{\mathrm{i,f}} \sim Z_{\mathrm{eff}}^{-2}$ [23, 25]. Therefore, the lifetimes of Rydberg states are expected to follow the Hydrogenic scaling law [25]

$$\tau(Z_{\mathrm{eff}}) \propto Z_{\mathrm{eff}}^{-4}\,, \tag{1}$$

which predicts that the lifetime of Rydberg states in singly charged ions is reduced by a factor of 16 compared to the lifetime of Rydberg states in neutral atoms.

In this work, we show that certain low angular momentum Rydberg series in alkaline-earth metal ions do not follow the scaling law (1), but are significantly larger than expected, even reaching the lifetime values of Rydberg states of neutral atoms. Therefore, we refer to lifetimes that do not follow (1) as *anomalously enhanced*. As an illustration of this enhancement we systematically compare the lifetimes of ^{85}Rb and ^{88}Sr^{+} and show that at zero temperature Rydberg P states are anomalously long-lived. This anomaly is caused by an accidental cancellation in the transition matrix elements of the relevant decay pathways. Interestingly, this anomalous longevity persists even at room temperature. Here, the anomaly is underpinned by the enlarged energetic separation of ionic Rydberg levels compared to those of neutral atoms.

Calculation of Rydberg state lifetimes. In this section, we describe how we numerically compute the lifetimes of Rydberg states in alkali-metal atoms (Group I) and alkaline-earth metal ions (Group II). For concreteness, we focus on ^{85}Rb and ^{88}Sr^{+}, both employed in experiments with Rydberg atoms and ions [25, 33]. These two species are part of the same isoelectronic sequence [Kr]5s^{1}, such

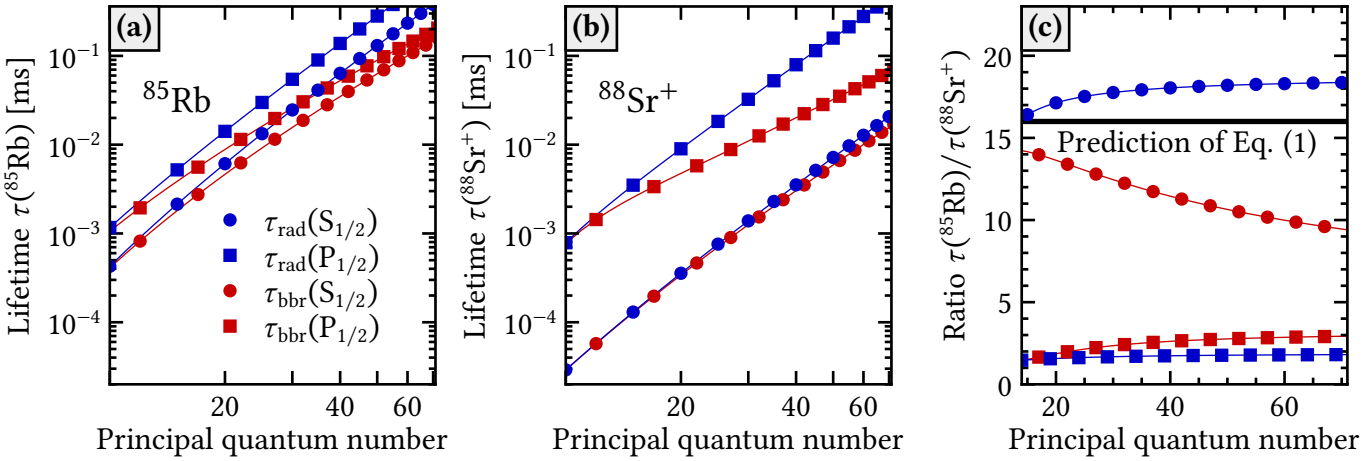

Figure 1. **Rydberg-state lifetimes.** (a) Numerically computed lifetimes of Rydberg S (dots) and P (squares) states of ^{85}Rb. Blue and red data show the radiative ($T = 0\,\mathrm{K}$) lifetimes (3), τ_{rad}, and the room-temperature ($T = 300\,\mathrm{K}$) lifetimes (4), τ_{bbr}, respectively. The data points are connected to guide the eye. (b) Analogous plot to panel (a) but for $^{88}\mathrm{Sr}^+$. (c) Comparison of lifetimes. The panel shows the ratio $\tau(^{85}\mathrm{Rb})/\tau(^{88}\mathrm{Sr}^+)$ between the lifetimes $\tau(^{85}\mathrm{Rb})$ and $\tau(^{88}\mathrm{Sr}^+)$ of Rydberg states in ^{85}Rb and $^{88}\mathrm{Sr}^+$. The Hydrogenic scaling law (1) predicts the constant ratio of 16, indicated by the black horizontal line. The lifetimes shown in panels (a) and (b) are tabulated in the Supplemental Material (SM) [26] and can be compared to numerical calculations of Rydberg-state lifetimes for neutral Group-I and singly charged Group-II elements conducted in Refs. [27–32]. Benchmarks of the numerically computed lifetimes for ^{85}Rb against experimental data can be found in the End Matter (EM).

that their electronic properties can be compared directly.

To numerically compute the lifetimes of the relevant Rydberg levels, we start by computing the eigenenergies and eigenstates for both ^{85}Rb and $^{88}\mathrm{Sr}^+$. This is done by diagonalising the following single-electron model Hamiltonian that describes the dynamics of the valence electron:

$$H_{\mathrm{val}} = \frac{\boldsymbol{p}^2}{2m} + V_s(r)\,. \tag{2}$$

The first term is the kinetic energy of the valence electron with mass m. The second term is a so-called *parametric model potential* V_s, which depends on the atom or ion species $s = {}^{85}\mathrm{Rb}, {}^{88}\mathrm{Sr}^+$. This potential accounts for the fact that the nucleus is 'screened' by the ground-state electron cloud. The size of the electron cloud is characterised by the cutoff radius r_{c} [34, 35]. At distances $r \gg r_{\mathrm{c}}$, the valence electron experiences the Coulomb potential $V_s(r \gg r_{\mathrm{c}}) \approx -Z_{\mathrm{eff}}e^2/(4\pi\varepsilon_0 r)$. Inside the effective nucleus, where $r \lesssim r_{\mathrm{c}}$, V_s includes short-ranged corrections. These corrections account for the electric polarisability of the electron cloud, its finite-size characterised by r_{c}, and the gradual transition between a Coulomb potential associated with the nuclear charge Z and the effective charge Z_{eff}, as r increases far beyond the cutoff radius r_{c} [23, 34, 35]. In this work we employ the parametric model potentials V_s from Refs. [34, 35] together with the spin-orbit interaction used in Ref. [19], which follows from relativistic perturbation theory [36]. To numerically diagonalise the Hamiltonian we use the software *AlkCalc* [37].

With the numerical results for the eigenenergies and the eigenstates we compute the lifetimes as follows: at zero temperature and within the dipole approximation, the inverse radiative lifetime τ_{rad}^{-1} of the initial Rydberg state $|\mathrm{i}\rangle$ is given by the inverse sum of Einstein-A coefficients [23]:

$$\tau_{\mathrm{rad}}^{-1} = \sum_{\mathrm{f}} A_{\mathrm{i}\to\mathrm{f}}\,, \quad \frac{\hbar}{E_{\mathrm{H}}} A_{\mathrm{i}\to\mathrm{f}} = \frac{4}{3}(2\pi)^3 F_{l_{\mathrm{i}},l_{\mathrm{f}}} \frac{a_{\mathrm{B}}\mu_{\mathrm{i,f}}^2}{\lambda_{\mathrm{i,f}}^3}\,. \tag{3}$$

The Einstein-A coefficient $A_{\mathrm{i}\to\mathrm{f}}$ [38] is the rate at which the initial state $|\mathrm{i}\rangle$ at energy E_{i} decays to the final electronic state $|\mathrm{f}\rangle$ at energy $E_{\mathrm{f}} < E_{\mathrm{i}}$. Further, $\alpha \approx 1/137$ is the fine-structure constant, $a_{\mathrm{B}} \approx 53\,\mathrm{pm}$ is Bohr's radius, $\lambda_{\mathrm{i,f}} = hc/|E_{\mathrm{f}} - E_{\mathrm{i}}|$ is the wavelength of the photon emitted upon decay, $\hbar = h/(2\pi)$ is the reduced Planck constant, and E_{H} is the Hartree energy unit [23]. The factor $F_{l_{\mathrm{i}},l_{\mathrm{f}}}$ stems from the angular part of the dipole transitions matrix element and depends on the orbital angular momentum quantum numbers l_{i} and l_{f} of the initial and the final states. It can be calculated using SU(2) angular momentum algebra relations stated in Ref. [39]. Finally, $\mu_{\mathrm{i,f}}$ in Eq. (3) is the radial dipole transition matrix element [24] between the initial and the final state.

In a room-temperature (black-body) environment ($T = 300\,\mathrm{K}$) the average number of photons with wavelength λ at temperature T is $N_{\mathrm{ph}}(\lambda, T) = [\exp(hc/[k_{\mathrm{B}}T\lambda]) - 1]^{-1}$. These photons cause radiative transitions from the initial Rydberg state $|\mathrm{i}\rangle$ to other Rydberg states $|\mathrm{f}\rangle$, both lower ($E_{\mathrm{f}} < E_{\mathrm{i}}$) and higher ($E_{\mathrm{f}} > E_{\mathrm{i}}$) in energy. Such transitions depopulate the initial Rydberg state and thereby reduce the radiative lifetime (3). The total lifetime τ_{bbr}, reduced by black-

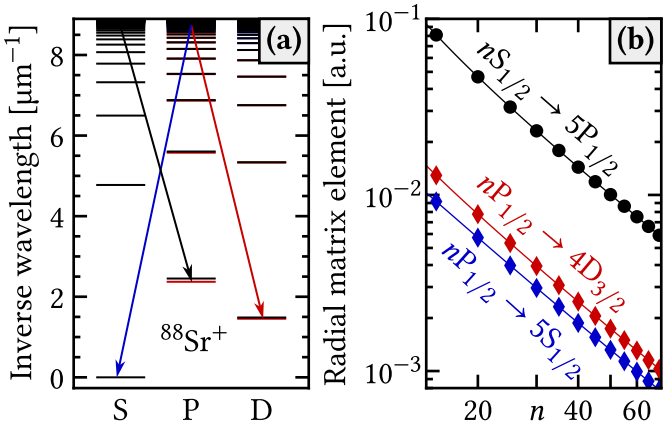

Figure 2. **Electronic spectrum and transition matrix elements of ^{88}Sr$^+$.** (a) Electronic bound-state spectrum. Red levels show the energy for $j = |l - 1/2|$ and black levels for $j = l + 1/2$. Arrows indicate the dominant radiative decay channels for the Rydberg S and P manifolds. (b) Radial transition dipole matrix elements [24] $\mu_{\mathrm{i,f}}$ [cf. Eq. (3)] as a function of the principal quantum number. For each decay channel in panel (a) the radial dipole matrix elements are shown. The colours indicate to which decay channel (arrows) in panel (a) the matrix elements correspond to. Dots and diamonds correspond to transitions out of the Rydberg S and P manifolds, respectively. The data points are connected to guide the eye.

body radiation, is calculated via [23]

$$\tau_{\mathrm{bbr}}^{-1} = \tau_{\mathrm{rad}}^{-1} + \sum_{\mathrm{f}} N_{\mathrm{ph}}(\lambda_{\mathrm{i,f}}, T) A_{\mathrm{i}\to\mathrm{f}}\,, \tag{4}$$

where the sum is over all possible final states $|\mathrm{i}\rangle$, both higher and lower in energy than $|\mathrm{i}\rangle$.

To benchmark the numerically computed lifetimes we compare them in the End Matter (EM) to experimental results for ^{85}Rb at room temperature. Since the results agree well with the experimental data, we have confidence in our numerical method [37].

Anomalously enhanced lifetimes. In the following we show that certain low angular momentum Rydberg series have anomalously enhanced lifetimes, for which the Hydrogenic scaling law (1) breaks down. For concreteness, we focus on ^{88}Sr$^+$, which is currently employed in experiments with Rydberg ions [25]. However, in the Supplemental Material (SM) [26] we tabulate lifetimes and give formulas to calculate them for ^{88}Sr$^+$, ^{40}Ca$^+$, and ^{85}Rb. These results show that also for ^{40}Ca$^+$, an isotope employed in Ref. [6], Rydberg P states can have lifetimes up to ∼20 times as high as S states with the same principal quantum number. For simplicity, we focus on the experimentally relevant [6, 25] Rydberg states $n\mathrm{S}_{1/2}$ and $n\mathrm{P}_{1/2}$. The discussion is split into two parts: first, we discuss the radiative lifetimes at zero-temperature, relevant for experiments in cryogenic environments [40, 41]. Subsequently, we focus on lifetimes in a room-temperature environment.

At zero temperature, we find that Rydberg P states have anomalously enhanced radiative lifetimes. This can be seen in the following way: the lifetimes for ^{85}Rb in Fig. 1(a) [blue data] show that Rydberg S and P states have similar lifetimes. In contrast, the lifetimes for ^{88}Sr$^+$ in Fig. 1(b) [blue data] show that S states (blue dots) have much shorter lifetimes than P states (blue squares). To test the scaling law (1) we plot the ratios $\tau(^{85}\mathrm{Rb})/\tau(^{88}\mathrm{Sr}^+)$ of the lifetimes in Fig. 1(c) [blue data]. The numerical data shows that Rydberg S states approximately follow the scaling law (1), while ionic Rydberg P states have much longer lifetimes than predicted. This is indicated by the fact that the ratios for S states (blue dots) lie close to the predicated constant value of 16, whereas for P states (blue squares) the ratio is much closer to unity. Therefore, we refer to the ionic Rydberg P-state lifetimes as *anomalously enhanced*.

In a room temperature environment at $T = 300\,\mathrm{K}$, we find that both Rydberg S and P states have anomalously enhanced lifetimes. To illustrate this we show in Figs. 1(a) and (b), analogously to the zero-temperature case, the lifetimes of Rydberg S (red dots) and Rydberg P (red squares) states in ^{85}Rb and ^{88}Sr$^+$. Computing the ratio $\tau(^{85}\mathrm{Rb})/\tau(^{88}\mathrm{Sr}^+)$ [red data in Fig. 1(c)] indeed shows that the lifetimes of both Rydberg S *and* Rydberg P states is anomalously enhanced, and the enhancement of the S-state lifetime even grows with the principal quantum number. The latter is evident by the fact that the ratios of the S-state lifetimes (red dots) decrease far below the prediction of Eq. (1). In the remainder of this work, we shed light on the enhancement mechanisms underlying the anomalous lifetime enhancement at zero and room temperature.

Enhancement mechanism at zero temperature. At zero temperature, the anomalously enhanced lifetimes of ionic Rydberg P states occurs due to accidental cancellations of the dipole transition matrix elements relevant for spontaneous emission. To rationalise this, we recall that the lifetime is given by the inverse sum over the Einstein-A coefficients $A_{\mathrm{i}\to\mathrm{f}}$ — the decay rates from the Rydberg state $|\mathrm{i}\rangle$ to the final states $|\mathrm{f}\rangle$. These coefficients scale as $A_{\mathrm{i}\to\mathrm{f}} \sim \mu_{\mathrm{i,f}}^2 \lambda_{\mathrm{i,f}}^{-3}$ [23, 24] with the radial transition matrix element $\mu_{\mathrm{i,f}}$ [24] and the wavelength $\lambda_{\mathrm{i,f}}$ of the photon emitted upon decay. A consequence of the scaling with the wavelength $\lambda_{\mathrm{i,f}}$ is that the dominant decay channels for spontaneous emission are transitions to low-lying electronic states [24]. In the bound-state energy spectrum of ^{88}Sr$^+$ in Fig. 2(a) the dominant channels for the relevant Rydberg S and P states are indicated by the black, blue, and red arrows. The radial transition matrix elements in panel (b), associated with the three decay channels, show that the transition matrix elements for decay of P states are indeed approximately an order of magnitude smaller compared to those of S states. The small matrix elements $\mu_{\mathrm{i,f}}$ suppress the Einstein-A coefficients $A_{\mathrm{i}\to\mathrm{f}} \sim \mu_{\mathrm{i,f}}^2$

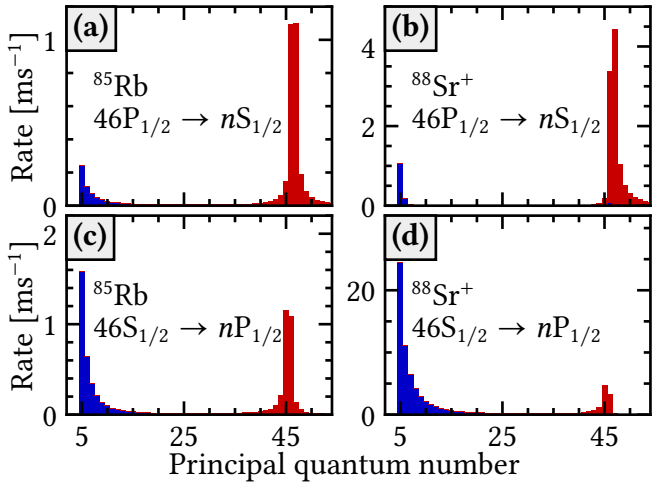

Figure 3. **Rydberg-state depopulation rates.** (a) Depopulation rates of the Rydberg state $46\mathrm{P}_{1/2}$ to the states $n\mathrm{S}_{1/2}$ in ^{85}Rb. The decay rate for spontaneous emission, $A_{\mathrm{i}\to\mathrm{f}}$, is shown in blue. The depopulation rates $N_{\mathrm{ph}}(\lambda_{\mathrm{i,f}},T)A_{\mathrm{i}\to\mathrm{f}}$ associated with transitions induced by black-body radiation are shown in red, where $N_{\mathrm{ph}}(\lambda_{\mathrm{i,f}},T)$ is the average number of photons with wavelength $\lambda_{\mathrm{i,f}}$ at temperature T. (b) Same as in (a) but for $^{88}\mathrm{Sr}^+$. (c) Same as in (a) but for transitions depopulating the Rydberg S state. (d) Same as in (c) but for $^{88}\mathrm{Sr}^+$.

and thus lead to the anomalously enhanced lifetimes of Rydberg P states shown in Figs. 1(b) and (c).

Interestingly, the scaling of the Einstein-A coefficients $A_{\mathrm{i}\to\mathrm{f}}\sim\lambda_{\mathrm{i,f}}^{-3}$ decreases the Rydberg P-state lifetime compared to that of S states. This can be seen by the fact that the inverse wavelengths $\lambda_{\mathrm{i,f}}^{-1}$ associated with the dominant decay channels for Rydberg S states (black arrow) are smaller compared to the inverse wavelengths of the relevant channels for P states (blue and red arrows). However, the numerical results in Fig. 1(b) show that ionic Rydberg P states have longer lifetimes than S states. This shows that the accidental cancellations in the matrix elements not only compensate this effect, but even enhance the lifetimes of ionic Rydberg P states beyond those of Rydberg S states.

We remark that the accidental cancellation in the matrix elements shown in Fig. 2(b) aligns well with experimental observations reported in the literature: Lange *et al.* [42] observed near-zero oscillator strengths for the transitions to Rydberg P states in singly charged Strontium. Further, Jones and Gallagher [43] observed the same phenomenon in singly charged Barium, which they could attribute to a zero in the radial transition dipole matrix element. Finally, we remark that the small matrix elements are not a *Cooper minimum* [44] — an accidental cancellation of the transition matrix element that only appears for certain principal quantum numbers. The anomaly shown by our results is stronger: the cancellation is consistently present across the *whole* range of considered principal quantum numbers.

Enhancement mechanism at room temperature. In a room-temperature environment the ratios in Fig. 1(c) show that the lifetimes of both Rydberg S and P states are anomalously enhanced, i.e., do not follow the Hydrogenic scaling law (1). This is caused by an increased energetic separation of ionic Rydberg energy levels compared to neutral atoms. To shed light on this, we first focus on Rydberg P states and show their depopulation rates for ^{85}Rb and $^{88}\mathrm{Sr}^+$ in Fig. 3(a) and (b), respectively. The room-temperature lifetime of Rydberg P states is dominated by transitions induced by black-body radiation. This can be seen by the fact that the depopulation rates $N_{\mathrm{ph}}(\lambda_{\mathrm{i,f}},T)A_{\mathrm{i}\to\mathrm{f}}$ associated with transitions induced by black-body radiation (red bars), dominate the spontaneous emission rates $A_{\mathrm{i}\to\mathrm{f}}$ (blue bars). Therefore, according to Eq. (4), the total lifetime of Rydberg P states can be approximated as

$$\tau_{\mathrm{bbr}}^{-1} \approx \sum_{\mathrm{f}} N_{\mathrm{ph}}(\lambda_{\mathrm{i,f}},T)A_{\mathrm{i}\to\mathrm{f}} \propto N_{\mathrm{ph}}(\lambda_{\mathrm{i,f}},T)Z_{\mathrm{eff}}^4 \,. \quad (5)$$

At the wavelengths $\lambda_{\mathrm{i,f}}$ relevant for transitions between Rydberg states, the average number of photons is well approximated as $N_{\mathrm{ph}}(\lambda_{\mathrm{i,f}},T) \approx \lambda_{\mathrm{i,f}}k_{\mathrm{B}}T/(hc) \propto Z_{\mathrm{eff}}^{-2}$, where k_{B} is Boltzmann's constant, c is the speed of light, and h is Planck's constant. Inserting this result into Eq. (5) yields the following scaling law for lifetimes dominated by black-body radiation:

$$\tau_{\mathrm{bbr}} \propto Z_{\mathrm{eff}}^{-2} \,. \quad (6)$$

This predicts that for Rydberg P states $\tau(^{85}\mathrm{Rb})/\tau(^{88}\mathrm{Sr}^+) \approx 4$, which is consistent with the data in Fig. 1(c) [red squares], showing a ratio of approximately 3.

Finally, we consider Rydberg S states, whose rates for spontaneous emission and depopulation through black-body radiation are exemplarily shown for S-P transitions in Figs. 3(c) and (d). In contrast to the P states, the lifetimes of the S states are not dominated by transitions to nearby Rydberg states due to black-body radiation and the scaling law (6). Nevertheless, there is a weak enhancement over the Hydrogenic scaling law (1).

Summary and outlook. Certain low angular momentum Rydberg series in singly charged alkaline-earth metal ions have unexpectedly long lifetimes, which can even become comparable to those of neutral atoms. Here, we have shed light on the mechanisms underlying this anomalous lifetime enhancement in both zero- and room-temperature environments. An important question is how this longevity can be exploited to enhance quantum computation and simulation protocols. For this it will be important to understand how much of this property persists in the presence of strong electromagnetic fields, since ions are typically confined in Paul [45] or Penning [46] traps. The latter feature magnetic flux densities on

the order of few Tesla, which drastically alters the electronic bound-state structure of the trapped Rydberg ions [47–51].

Acknowledgements. S.E. thanks W. S. Martins and J. W. P. Wilkinson for fruitful discussions on Rydberg ions. This work was supported by the European Union through the ERC grant OPEN-2QS (Grant No. 101164443) and the Deutsche Forschungsgemeinschaft within the research unit FOR 5413 (Grant No. 465199066). We also acknowledge funding through JST-DFG 2024: Japanese-German Joint Call for Proposals on "Quantum Technologies" (Japan-JST-DFG-ASPIRE 2024) under JST Grand No. JPMJAP24C2 and DFG Grant No. 554561799. W.L. acknowledges financial support from the EPSRC (Grant No. EP/W015641/1).

Data availability. The data and code that support the findings of this work are openly available [52].

AI usage statement. The authors used *Anthropic*'s *Claude (Sonnet 4)* for grammar and spell-checking of the manuscript. All suggestions were reviewed and approved by the authors. Further, it was used to extract experimentally measured lifetimes from a publication, which are plotted in the End Matter (please see the EM for details).

[1] T. F. Gallagher, Rydberg atoms, Reports on Progress in Physics **51**, 143 (1988).
[2] M. Saffman, T. G. Walker, and K. Mølmer, Quantum information with Rydberg atoms, Reviews of Modern Physics **82**, 2313 (2010).
[3] N. Šibalić and C. S. Adams, *Rydberg Physics*, 2399-2891 (IOP Publishing, 2018).
[4] A. Browaeys and T. Lahaye, Many-body physics with individually controlled Rydberg atoms, Nature Physics **16**, 132 (2020).
[5] M. Müller, L. Liang, I. Lesanovsky, and P. Zoller, Trapped Rydberg ions: from spin chains to fast quantum gates, New Journal of Physics **10**, 093009 (2008).
[6] F. Schmidt-Kaler, T. Feldker, D. Kolbe, J. Walz, M. Müller, P. Zoller, W. Li, and I. Lesanovsky, Rydberg excitation of trapped cold ions: a detailed case study, New Journal of Physics **13**, 075014 (2011).
[7] M. Mallweger, N. Kuk, V. Shankar, R. Thomm, H. Parke, I. Straka, W. Li, I. Lesanovsky, and M. Hennrich, Probing electronic state-dependent conformational changes in a trapped Rydberg ion Wigner crystal, arXiv **[quant-ph]**, 2507.23631 (2025).
[8] F. Pokorny, *A microwave dressed Rydberg ion*, Ph.D. thesis, Stockholm University (2020).
[9] F. Pokorny, C. Zhang, G. Higgins, and M. Hennrich, Magic trapping of a Rydberg ion with a diminished static polarizability, arXiv **[physics.atom-ph]**, 2005.12422 (2020).
[10] F. M. Gambetta, C. Zhang, M. Hennrich, I. Lesanovsky, and W. Li, Exploring the Many-Body Dynamics Near a Conical Intersection with Trapped Rydberg Ions, Physical Review Letters **126**, 233404 (2021).
[11] M. Chaudhary, R. Nath, and W. Li, Spin–Phonon Relaxation Dynamics from a Conical Intersection of Trapped Rydberg Ions, Photonics **11**, 1135 (2024).
[12] A. Belfakir and W. Li, Exploring vibronic dynamics near a sloped conical intersection with trapped Rydberg ions, Physical Review A **113**, 023323 (2026).
[13] A. Belfakir, Y. Bouasria, H. Rabitz, and A. Ratnani, Directional motional control via engineered conical intersections in trapped Rydberg ions, Physical Review A **113** (2026).
[14] A. Belfakir, Y. Bouasria, H. Rabitz, and A. Ratnani, Entanglement in trapped Rydberg ions via engineered conical intersections and addressing of individual-ions, Annals of Physics **494**, 170617 (2026).
[15] S. Euchner, M. B. M. Svendsen, and I. Lesanovsky, Nonequilibrium exciton dynamics in tailored molecular potentials of Rydberg ion crystals, arXiv **[physics.atom-ph]**, 2605.21250 (2026).
[16] J. W. P. Wilkinson, W. Li, and I. Lesanovsky, Spectral Signatures of Vibronic Coupling in Trapped Cold Ionic Rydberg Systems, Physical Review Letters **132**, 223401 (2024).
[17] W. Li and I. Lesanovsky, Entangling quantum gate in trapped ions via Rydberg blockade, Applied Physics B **114**, 37 (2014).
[18] C. Zhang, F. Pokorny, W. Li, G. Higgins, A. Pöschl, I. Lesanovsky, and M. Hennrich, Submicrosecond entangling gate between trapped ions via Rydberg interaction, Nature **580**, 345 (2020).
[19] J. W. P. Wilkinson, K. Bolsmann, T. L. M. Guedes, M. Müller, and I. Lesanovsky, Two-qubit gate protocols with microwave-dressed Rydberg ions in a linear Paul trap, New Journal of Physics **27**, 064502 (2025).
[20] Z.-C. Mao, Y.-Z. Xu, Q.-X. Mai, W.-D. Zhao, Y. Jiang, Y. Wang, X.-Y. Chang, L. He, L. Yao, Z.-C. Zhou, Y.-K. Wu, and L.-M. Duan, Experimental Realization of Multi-ion Sympathetic Cooling on a Trapped Ion Crystal, Physical Review Letters **127**, 143201 (2021).
[21] V. So, M. D. Suganthi, A. Menon, M. Zhu, R. Zhuravel, H. Pu, P. G. Wolynes, J. N. Onuchic, and G. Pagano, Trapped-ion quantum simulation of electron transfer models with tunable dissipation, Science Advances **10**, eads8011 (2024).
[22] V. So, M. D. Suganthi, M. Zhu, A. Menon, G. Tomaras, R. Zhuravel, H. Pu, P. G. Wolynes, J. N. Onuchic, and G. Pagano, Quantum simulation of charge and exciton transfer in multi-mode models using engineered reservoirs, Nature Communications **17**, 438 (2026).
[23] H. Friedrich, *Theoretical Atomic Physics*, 4th ed., Graduate Texts in Physics (Springer Cham, 2017).
[24] N. Šibalić, J. D. Pritchard, C. S. Adams, and K. J. Weatherill, ARC: An open-source library for calculating properties of alkali Rydberg atoms, Computer Physics Communications **220**, 319 (2017).
[25] G. Higgins, *A Single Trapped Rydberg Ion*, 1st ed., Springer Theses (Springer Cham, 2019).
[26] S. Euchner, W. Li, and I. Lesanovsky, See the Supplemental Material (SM) for tables with lifetimes and formulas for lifetimes of Rydberg states in the Calcium and Strontium ion and the Rubidium atom. The SM includes the additional References [56–58].
[27] C. E. Theodosiou, Lifetimes of alkali-metal-atom Rydberg states, Physical Review A **30**, 2881 (1984).
[28] X. He, B. Li, A. Chen, and C. Zhang, Model-potential

calculation of lifetimes of Rydberg states of alkali atoms, Journal of Physics B: Atomic, Molecular and Optical Physics **23**, 661 (1990).

[29] I. I. Beterov, I. I. Ryabtsev, D. B. Tretyakov, and V. M. Entin, Quasiclassical calculations of blackbody-radiation-induced depopulation rates and effective lifetimes of Rydberg ns, np, and nd alkali-metal atoms with $n \leq 80$, Physical Review A **79**, 052504 (2009).

[30] I. I. Beterov, I. I. Ryabtsev, D. B. Tretyakov, and V. M. Entin, Erratum: Quasiclassical calculations of blackbody-radiation-induced depopulation rates and effective lifetimes of Rydberg ns, np, and nd alkali-metal atoms with $n \leq 80$ [Phys. Rev. A **79**, 052504 (2009)], Physical Review A **80**, 059902 (2009).

[31] I. L. Glukhov, E. A. Nikitina, and V. D. Ovsiannikov, Lifetimes of Rydberg States in Ions of the Group II Elements, Optics and Spectroscopy **115**, 9 (2013).

[32] I. L. Glukhov, E. A. Nikitina, and V. D. Ovsiannikov, Blackbody-radiation-induced shifts and the broadening of Rydberg states in the ions of group IIa elements, Journal of Physics B: Atomic, Molecular and Optical Physics **49**, 035003 (2016).

[33] V. Bendkowsky, B. Butscher, J. Nipper, J. P. Shaffer, R. Löw, and T. Pfau, Observation of ultralong-range Rydberg molecules, Nature **458**, 1005 (2009).

[34] M. Marinescu, H. R. Sadeghpour, and A. Dalgarno, Dispersion coefficients for alkali-metal dimers, Physical Review A **49**, 982 (1994).

[35] M. Aymar, C. H. Greene, and E. Luc-Koenig, Multichannel Rydberg spectroscopy of complex atoms, Reviews of Modern Physics **68**, 1015 (1996).

[36] E. U. Condon and G. H. Shortley, *The Theory of Atomic Spectra*, 2nd ed. (Cambridge University Press, 1951).

[37] S. Euchner, *AlkCalc*: Alkali-metal atom and alkaline-earth-metal ion calculator (v5.0), GitHub Repository: https://github.com/simon-euchner/AlkCalc.

[38] A. Einstein, Zur quantentheorie der strahlung, Physikalische Zeitschrift **XVIII**, 121 (1917).

[39] D. A. Varshalovich, A. N. Moskalev, and V. K. Khersonskii, *Quantum Theory of Angular Momentum* (WORLD SCIENTIFIC, 1988).

[40] G. Pagano, P. W. Hess, H. B. Kaplan, W. L. Tan, P. Richerme, P. Becker, A. Kyprianidis, J. Zhang, E. Birckelbaw, M. R. Hernandez, Y. Wu, and C. Monroe, Cryogenic trapped-ion system for large scale quantum simulation, Quantum Science and Technology **4**, 014004 (2018).

[41] Z. Zhang, T.-W. Hsu, T. Y. Tan, D. H. Slichter, A. M. Kaufman, M. Marinelli, and C. A. Regal, High Optical Access Cryogenic System for Rydberg Atom Arrays with a 3000-Second Trap Lifetime, PRX Quantum **6**, 020337 (2025).

[42] V. Lange, M. A. Khan, U. Eichmann, and W. Sandner, Rydberg states of the strontium ion, Zeitschrift für Physik D — Atoms, Molecules and Clusters **18**, 319 (1991).

[43] R. R. Jones and T. F. Gallagher, Observation of Ba^+ $np_{1/2}$ and ng_j Rydberg series, Journal of the Optical Society of America B **6**, 1467 (1989).

[44] I. I. Beterov, C. W. Mansell, E. A. Yakshina, I. I. Ryabtsev, D. B. Tretyakov, V. M. Entin, C. MacCormick, M. J. Piotrowicz, A. Kowalczyk, and S. Bergamini, Cooper minima in the transitions from low-excited and Rydberg states of alkali-metal atoms, arXiv **[physics.atom-ph]**, 1207.3626 (2012).

[45] W. Paul, Electromagnetic traps for charged and neutral particles, Reviews of Modern Physics **62**, 531 (1990).

[46] M. Vogel, *Particle Confinement in Penning Traps*, 2nd ed., edited by G. W. F. Drake, Springer Series on Atomic, Optical, and Plasma Physics, Vol. 126 (Springer, 2024).

[47] S. K. Knudson and D. W. Noid, Spectra of atomic Rydberg states in strong magnetic fields, Chemical Physics **89**, 353 (1984).

[48] G. Wunner, M. Kost, and H. Ruder, "Circular" states of Rydberg atoms in strong magnetic fields, Physical Review A **33**, 1444(R) (1986).

[49] G. Wunner and H. Ruder, Atoms in strong magnetic fields, Physica Scripta **36**, 291 (1987).

[50] T. Pohl, H. R. Sadeghpour, and P. Schmelcher, Cold and ultracold Rydberg atoms in strong magnetic fields, Physics Reports **484**, 181 (2009).

[51] W. S. Martins, M. Hennrich, F. Schmidt-Kaler, and I. Lesanovsky, Quantum simulation with Rydberg ions in a Penning trap, arXiv **[quant-ph]**, 2601.01626 (2026).

[52] S. Euchner, Data and code for 'Anomalously enhanced lifetimes of low angular momentum Rydberg states in singly charged alkaline-earth metal ions' [Dataset], Zenodo (2026), `https://doi.org/10.5281/zenodo.22878408`.

[53] D. B. Branden, T. Juhasz, T. Mahlokozera, C. Vesa, R. O. Wilson, M. Zheng, A. Kortyna, and D. A. Tate, Radiative lifetime measurements of rubidium Rydberg states, Journal of Physics B: Atomic, Molecular and Optical Physics **43**, 015002 (2010).

[54] M. Archimi, C. Simonelli, L. Di Virgilio, A. Greco, M. Ceccanti, E. Arimondo, D. Ciampini, I. I. Ryabtsev, I. I. Beterov, and O. Morsch, Measurements of single-state and state-ensemble lifetimes of high-lying Rb Rydberg levels, Physical Review A **100**, 030501(R) (2019).

[55] G. Simons, New Model Potential for Pseudopotential Calculations, Journal of Chemical Physics **55**, 756 (1971).

[56] W. Li, I. Mourachko, M. W. Noel, and T. F. Gallagher, Millimeter-wave spectroscopy of cold Rb Rydberg atoms in a magneto-optical trap: Quantum defects of the ns, np, and nd series, Phys. Rev. A **67**, 052502 (2003).

[57] A. Mokhberi, J. Vogel, J. Andrijauskas, P. Bachor, J. Walz, and F. Schmidt-Kaler, Determination of quantum defect for the Rydberg P series of Ca II, Journal of Physics B: Atomic, Molecular and Optical Physics **52**, 214001 (2019).

[58] J. Andrijauskas, J. Vogel, A. Mokhberi, and F. Schmidt-Kaler, Rydberg Series Excitation of a Single Trapped $^{40}Ca^+$ Ion for Precision Measurements and Principal Quantum Number Scalings, Physical Review Letters **127**, 203001 (2021).

END MATTER

We benchmark our numerical method against experimental and numerical data from the literature. To our knowledge, reasonably large sets of experimentally measured Rydberg-state lifetimes exist only for the Rydberg states $n\mathrm{S}_{1/2}$, $n\mathrm{P}_{3/2}$, and $n\mathrm{D}_{5/2}$ in ^{85}Rb at room temperature. Figure 4 compares these measured lifetimes (black diamonds and grey stars) to the lifetimes predicted by

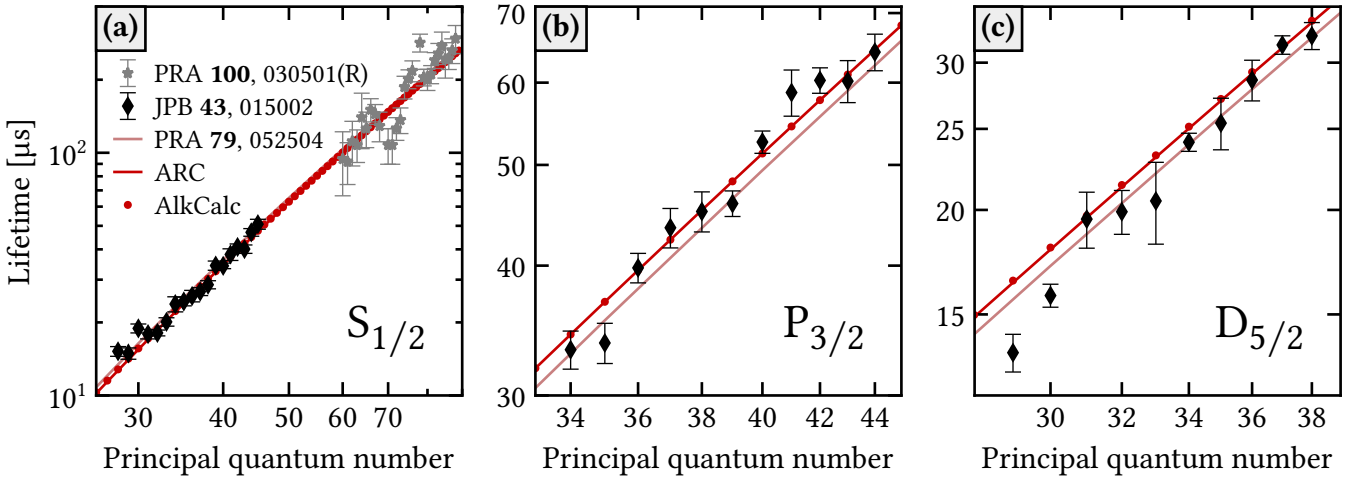

Figure 4. **Benchmark of room-temperature lifetimes of Rydberg states in ^{85}Rb.** (a) S-state lifetimes. Red dots show lifetimes of the Rydberg $n\mathrm{S}_{1/2}$ states in ^{85}Rb computed with *AlkCalc* [37]. Black diamonds show experimental results from Ref. [53] for ^{85}Rb. Grey stars show experimental results from Ref. [54]. In the latter case, the data shown here is not available in tabulated form. Therefore, we employed *Anthropic*'s *Claude (Sonnet 4)* to extract the data directly from the figure in the portable-document-format (PDF) file. We note that due to this method, the precision of the data and the associated error bars is not quantitatively known. However, the extracted data (grey stars) agrees well with our numerical prediction. We remark that for the extracted data the specific isotope of Rubidium is not specified. The red line shows the lifetimes computed with the software *ARC* [24]. Finally, the light red line shows results from Ref. [29, 30]. (b) P-state lifetimes. Same plot as in (a) but for the Rydberg states $n\mathrm{P}_{3/2}$. (c) D-state lifetimes. Same plot as in (a) but for the Rydberg states $n\mathrm{D}_{5/2}$.

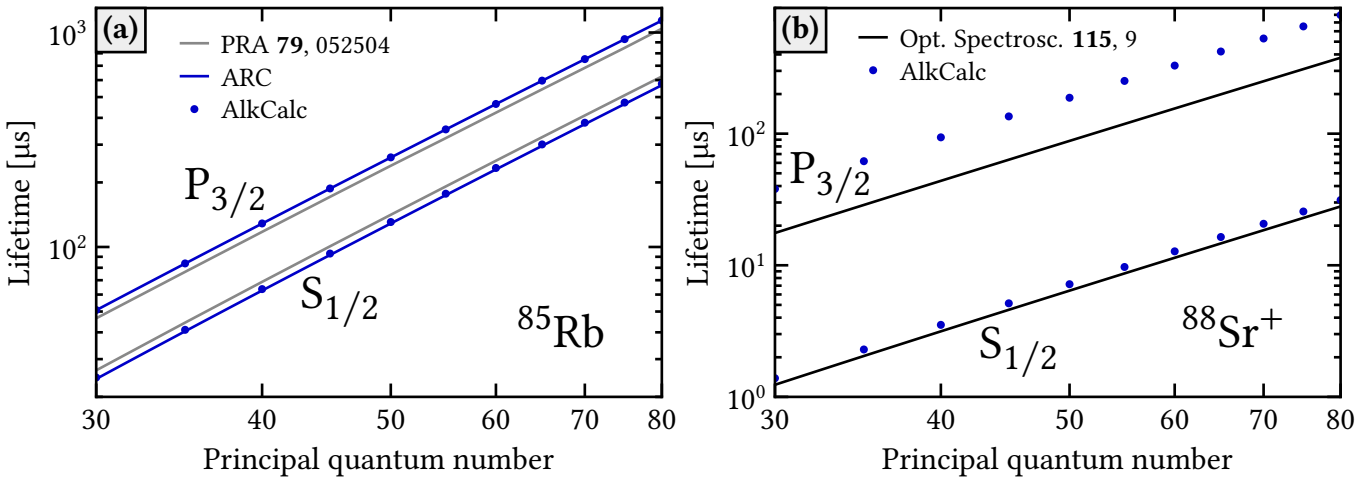

Figure 5. **Comparison of zero-temperature lifetimes of Rydberg states in ^{85}Rb and ^{88}Sr$^+$ to numerical results from the literature.** (a) Comparison of lifetimes obtained with *AlkCalc* [37] (blue dots) and *ARC* [24] (blue lines) to results from Ref. [44] (grey lines). The lifetimes are shown for S and P states in ^{85}Rb. (b) Comparison of lifetimes obtained with *AlkCalc* (blue dots) to results from Ref. [31] (black lines). The lifetimes are shown for S and P states in ^{88}Sr$^+$.

AlkCalc [37] (red dots), the software used in this work, as well to two other theoretical works from the literature: ARC [24] (red line) and Ref. [44] (light red line). All results agree well, except for a slight deviation of the lifetimes obtained in Ref. [44] from the predictions by *AlkCalc* and *ARC*. The deviation is visible by comparing the red and light red curves. Further, we benchmark the lifetimes computed with *AlkCalc* at zero temperature against theoretical lifetimes from Ref. [44] (grey line) and from ARC [24] (blue line). Figure 5(a) shows good agreement between our method, *ARC*, and Ref. [44], with the results from Ref. [44] again deviating slightly. Panel (b) shows the analogous comparison for ^{88}Sr$^+$. Note that for ^{88}Sr$^+$ the software *ARC* is unavailable since it is limited to alkali-metal atoms. Instead, we compare our results to the numerical data obtained in Ref. [31]. The S-state lifetimes agree better than the P-state lifetimes, though the anomalous enhancement of the P-state lifetimes re-

mains clearly visible also in the data from Ref. [31] (black lines).

A likely source of the quantitative discrepancy for the zero-temperature P-state lifetimes in $^{88}Sr^{+}$ is the model potential used for computing the eigenenergies and eigenstates: Ref. [31] uses Fuse's model [55]. This model potential, V, is given by the potential for Hydrogenic ions with the replacement $l \mapsto \nu_l$:

$$V(r) = -\frac{Z_{\text{eff}} e^2}{4\pi\varepsilon_0}\frac{1}{r} + \frac{\hbar^2 \nu_l(\nu_l+1)}{2mr^2}\,, \tag{7}$$

where ν_l is an l-dependent continuous parameter, optimised to reproduce the correct spectroscopic eigenenergies, and $Z_{\text{eff}} = 2$ is the effective nuclear charge. In contrast, the parametric model potential [35] employed by *AlkCalc* has a more sophisticated structure at small radii r with a larger set of independent parameters, optimised to match spectroscopic data. Therefore, we expect that the radial eigenstates computed with *AlkCalc* capture the complex small-r behaviour of the wave function more accurately than Fuse's model. This matters particularly for zero-temperature lifetimes, since the dominant transition matrix elements are between Rydberg states and low-lying electronic states. The latter typically penetrate the ground-state electron cloud and the nucleus deeply and are therefore highly sensitive to the small-r behaviour of the model potential. In particular for Rydberg P states, where the transition matrix elements show accidental cancellations, precisely reproducing the small-r behaviour of the radial wave function is especially important. Therefore, this explanation aligns well with the fact that the quantitative discrepancy is most pronounced for zero-temperature lifetimes of P states, as suggested by Fig. 5(b) (cf. blue dots and black lines).

Supplemental material for: Non-equilibrium exciton dynamics in tailored molecular potentials of Rydberg ion crystals

Simon Euchner[1], Weibin Li[2], and Igor Lesanovsky[1,2]

[1] *Institut für Theoretische Physik and Center for Integrated Quantum Science and Technology, Universität Tübingen, Auf der Morgenstelle 14, 72076 Tübingen, Germany*
[2] *School of Physics and Astronomy and Centre for the Mathematics and Theoretical Physics of Quantum Non-Equilibrium Systems, The University of Nottingham, Nottingham, NG7 2RD, United Kingdom*

In Sec. S1 we provide tables with numerically computed lifetimes of Rydberg states in $^{40}Ca^+$, $^{88}Sr^+$, and ^{85}Rb at zero temperature and room temperature. In Sec. S2 we provide formulas for calculating Rydberg-state lifetimes in $^{40}Ca^+$, $^{88}Sr^+$, and ^{85}Rb

S1. LIFETIMES OF RYDBERG STATES IN $^{40}Ca^+$, $^{88}Sr^+$, AND ^{85}Rb

In Tabs. S1, S2, and S3 numerically computed lifetimes are tabulated for the Calcium ion $^{40}Ca^+$ and the Strontium ion $^{88}Sr^+$, and the Rubidium atom ^{85}Rb, respectively. The lifetimes are computed at zero temperature, yielding the radiative lifetimes, $\tau_{\rm rad}$, and at room temperature $T = 300\,\mathrm{K}$, $\tau_{\rm bbr}$, yielding lifetimes that are reduced by black-body induced transitions. All lifetimes are calculated within the dipole approximation [23, 37]. As discussed in the main text, black-body radiation can depopulate Rydberg states by transitions to other Rydberg states that lie *higher* in energy than the level of interest. To account for this numerically, we truncate the electronic basis 30 states above the Rydberg level of interest, i.e., we consider black-body induced excitation of the Rydberg level $n\mathrm{L}_j$ up to and including the Rydberg level $(n+30)\mathrm{L}'_{j'}$.

S2. FORMULAS FOR CALCULATING LIFETIMES OF RYDBERG STATES

In this section we give simple formulas for calculating the Rydberg-state lifetimes of $^{40}Ca^+$, $^{88}Sr^+$, and ^{85}Rb given in Tabs. S1, S2, and S3. Following Ref. [29], the equation for the radiative (zero-temperature) lifetime is

$$\tau_{\rm rad}^{\rm model}[\mathrm{ns}] = \tau_s[\mathrm{ns}] \times n_{\rm eff}^{\delta}\,. \tag{S1}$$

Here, $n_{\rm eff} = n - \delta_{l,j}$ is the effective principal quantum number with the quantum defect $\delta_{l,j}$ [23]. The quantities τ_s and δ are fitting parameters. These parameters are obtained by fitting formula (S1) to the tabulated lifetimes. For the lifetimes reduced by black-body radiation at temperature $T = 300\,\mathrm{K}$, Ref. [29] states the formula

$$\tau_{\rm bbr}^{\rm model}[\mathrm{ns}] = \left(\frac{1}{\tau_{\rm rad}[\mathrm{ns}]} + \frac{A[\mathrm{ns}^{-1}]}{n_{\rm eff}^{D}}\frac{21.4}{\exp\big(315780\times B/(n_{\rm eff}^{C}\times T[\mathrm{K}])\big)-1}\right)^{-1}. \tag{S2}$$

Here, A, B, C, and D are fitting parameters. To compute these fitting parameters we apply the following procedure: we first compute τ_s and δ by fitting Eq. (S1) to the radiative lifetimes. Subsequently, we plug the resulting τ_s and δ into Eq. (S2) to reduce $\tau_{\rm bbr} = \tau_{\rm bbr}(A, B, C, D)$ to a sole function of the fitting parameters A, B, C, and D. By fitting this model to the lifetimes reduced by black-body radiation, we obtain the optimal values for A, B, C, and D. For the fit itself, we choose a least-squares cost function and minimize it. The results for the fitting parameters and the employed values for the quantum defects, $\delta_{l,j}$, are given in Tab. S4.

To quantify the quality of the fits, and thereby the formulas (S1) and (S2), we consider the maximal relative errors

$$\Delta_{\rm rad} = \max_{20\le n\le 80}\frac{|\tau_{\rm rad}^{\rm model}(n) - \tau_{\rm rad}(n)|}{\tau_{\rm rad}(n)} \tag{S3}$$

Table S1. **Lifetimes of Rydberg states in $^{40}Ca^{+}$.** Lifetimes calculated with *AlkCalc* [37] for principal quantum numbers $20 \leq n \leq 80$. Values are in microseconds (µs) and given to four significant digits. 'rad' denotes radiative ($T = 0\,\mathrm{K}$) lifetimes, while 'bbr' denotes room-temperature ($T = 300\,\mathrm{K}$) lifetimes, which are reduced by black-body-radiation-induced transitions.

n	$S_{\frac{1}{2}}$(rad)	$P_{\frac{1}{2}}$(rad)	$P_{\frac{3}{2}}$(rad)	$D_{\frac{3}{2}}$(rad)	$D_{\frac{5}{2}}$(rad)	$S_{\frac{1}{2}}$(bbr)	$P_{\frac{1}{2}}$(bbr)	$P_{\frac{3}{2}}$(bbr)	$D_{\frac{3}{2}}$(bbr)	$D_{\frac{5}{2}}$(bbr)
20	0.3882	8.472	9.013	0.5231	0.5299	0.3703	4.507	4.637	0.4936	0.4996
21	0.455	9.88	10.52	0.6085	0.6165	0.4319	5.001	5.139	0.5711	0.578
22	0.5291	11.44	12.18	0.7028	0.712	0.4997	5.52	5.666	0.6559	0.6638
23	0.6109	13.14	14.01	0.8064	0.817	0.5741	6.065	6.219	0.7485	0.7574
24	0.7007	15.01	16.01	0.9197	0.9318	0.6554	6.637	6.798	0.8489	0.8591
25	0.799	17.05	18.19	1.043	1.057	0.7437	7.235	7.404	0.9577	0.969
26	0.9061	19.27	20.56	1.177	1.193	0.8393	7.861	8.038	1.075	1.088
27	1.022	21.66	23.12	1.322	1.339	0.9425	8.515	8.699	1.201	1.215
28	1.148	24.25	25.89	1.478	1.498	1.054	9.197	9.389	1.336	1.351
29	1.284	27.04	28.87	1.647	1.668	1.173	9.908	10.11	1.48	1.497
30	1.43	30.03	32.07	1.827	1.851	1.3	10.65	10.85	1.634	1.653
31	1.587	33.23	35.5	2.02	2.047	1.436	11.42	11.63	1.797	1.818
32	1.755	36.66	39.16	2.227	2.256	1.58	12.21	12.44	1.971	1.994
33	1.935	40.31	43.07	2.447	2.479	1.734	13.04	13.27	2.155	2.179
34	2.126	44.19	47.23	2.681	2.716	1.896	13.9	14.14	2.349	2.376
35	2.329	48.32	51.65	2.929	2.968	2.069	14.79	15.03	2.554	2.583
36	2.546	52.7	56.33	3.193	3.235	2.25	15.7	15.96	2.77	2.801
37	2.775	57.33	61.29	3.471	3.517	2.442	16.65	16.91	2.997	3.03
38	3.017	62.23	66.53	3.766	3.816	2.643	17.63	17.9	3.235	3.271
39	3.274	67.4	72.06	4.077	4.131	2.855	18.64	18.92	3.485	3.524
40	3.544	72.85	77.9	4.404	4.462	3.077	19.67	19.96	3.747	3.788
41	3.829	78.59	84.03	4.748	4.811	3.309	20.74	21.04	4.02	4.064
42	4.129	84.62	90.49	5.11	5.178	3.553	21.84	22.15	4.306	4.353
43	4.444	90.95	97.26	5.49	5.563	3.807	22.97	23.29	4.604	4.654
44	4.775	97.58	104.4	5.888	5.966	4.072	24.13	24.45	4.915	4.968
45	5.122	104.5	111.8	6.305	6.389	4.349	25.32	25.65	5.238	5.295
46	5.485	111.8	119.6	6.741	6.831	4.637	26.54	26.88	5.575	5.635
47	5.865	119.4	127.7	7.197	7.292	4.937	27.8	28.14	5.924	5.988
48	6.263	127.4	136.2	7.673	7.775	5.248	29.08	29.43	6.287	6.354
49	6.677	135.7	145.1	8.169	8.278	5.572	30.39	30.75	6.664	6.734
50	7.11	144.3	154.4	8.687	8.802	5.908	31.74	32.11	7.053	7.128
51	7.561	153.3	164	9.225	9.348	6.256	33.11	33.49	7.457	7.535
52	8.031	162.7	174	9.786	9.916	6.616	34.52	34.9	7.875	7.957
53	8.52	172.4	184.5	10.37	10.51	6.989	35.95	36.35	8.307	8.393
54	9.028	182.6	195.3	10.97	11.12	7.375	37.42	37.82	8.753	8.844
55	9.556	193.1	206.6	11.6	11.76	7.774	38.92	39.33	9.214	9.309
56	10.1	204	218.2	12.26	12.42	8.186	40.44	40.86	9.689	9.788
57	10.67	215.3	230.4	12.93	13.1	8.611	42	42.43	10.18	10.28
58	11.26	227	242.9	13.63	13.81	9.049	43.59	44.03	10.68	10.79
59	11.88	239.2	255.9	14.36	14.55	9.501	45.21	45.66	11.2	11.32
60	12.51	251.8	269.4	15.11	15.31	9.966	46.86	47.32	11.74	11.86
61	13.16	264.8	283.3	15.89	16.1	10.45	48.55	49.01	12.29	12.41
62	13.84	278.2	297.7	16.69	16.91	10.94	50.26	50.73	12.86	12.98
63	14.54	292.1	312.6	17.52	17.75	11.45	52	52.48	13.44	13.57
64	15.27	306.5	327.9	18.37	18.62	11.97	53.78	54.26	14.04	14.17
65	16.01	321.3	343.8	19.26	19.51	12.5	55.58	56.07	14.65	14.79
66	16.79	336.6	360.2	20.17	20.44	13.05	57.42	57.92	15.28	15.43
67	17.58	352.4	377	21.11	21.39	13.62	59.28	59.79	15.92	16.08
68	18.4	368.6	394.4	22.08	22.37	14.2	61.18	61.7	16.59	16.75
69	19.25	385.4	412.4	23.08	23.38	14.79	63.11	63.63	17.27	17.43
70	20.12	402.6	430.8	24.1	24.42	15.4	65.06	65.6	17.96	18.13
71	21.02	420.4	449.8	25.16	25.5	16.02	67.05	67.59	18.67	18.85
72	21.94	438.6	469.4	26.25	26.6	16.66	69.07	69.62	19.4	19.59
73	22.89	457.4	489.5	27.37	27.73	17.31	71.12	71.68	20.15	20.34
74	23.87	476.7	510.2	28.52	28.9	17.98	73.21	73.77	20.91	21.11
75	24.87	496.6	531.4	29.7	30.09	18.67	75.32	75.89	21.69	21.89
76	25.91	517	553.3	30.91	31.33	19.37	77.46	78.04	22.49	22.7
77	26.97	538	575.7	32.16	32.59	20.08	79.63	80.22	23.3	23.52
78	28.06	559.5	598.7	33.44	33.89	20.82	81.84	82.43	24.13	24.36
79	29.18	581.6	622.4	34.76	35.22	21.56	84.07	84.67	24.98	25.21
80	30.32	604.2	646.6	36.1	36.58	22.33	86.34	86.95	25.85	26.09

Table S2. **Lifetimes of Rydberg states in $^{88}Sr^{+}$.** Lifetimes calculated with *AlkCalc* [37] for principal quantum numbers $20 \leq n \leq 80$. Values are in microseconds (µs) and given to four significant digits. 'rad' denotes radiative ($T = 0\,\mathrm{K}$) lifetimes, while 'bbr' denotes room-temperature ($T = 300\,\mathrm{K}$) lifetimes, which are reduced by black-body-radiation-induced transitions.

n	$S_{\frac{1}{2}}$(rad)	$P_{\frac{1}{2}}$(rad)	$P_{\frac{3}{2}}$(rad)	$D_{\frac{3}{2}}$(rad)	$D_{\frac{5}{2}}$(rad)	$S_{\frac{1}{2}}$(bbr)	$P_{\frac{1}{2}}$(bbr)	$P_{\frac{3}{2}}$(bbr)	$D_{\frac{3}{2}}$(bbr)	$D_{\frac{5}{2}}$(bbr)
20	0.3563	8.984	10.31	0.3677	0.3798	0.3397	4.745	5.009	0.3542	0.3654
21	0.4209	10.5	12.1	0.4299	0.4441	0.3992	5.25	5.531	0.4124	0.4254
22	0.493	12.19	14.09	0.4989	0.5153	0.4651	5.778	6.077	0.4766	0.4915
23	0.573	14.04	16.27	0.5748	0.5938	0.5377	6.332	6.647	0.5469	0.5639
24	0.6612	16.06	18.67	0.6581	0.6798	0.6172	6.912	7.243	0.6235	0.6428
25	0.758	18.28	21.29	0.7491	0.7738	0.7039	7.518	7.865	0.7068	0.7286
26	0.8639	20.68	24.14	0.8482	0.8761	0.798	8.152	8.514	0.7969	0.8214
27	0.9793	23.29	27.23	0.9556	0.9871	0.9	8.814	9.191	0.8941	0.9214
28	1.105	26.11	30.57	1.072	1.107	1.01	9.504	9.897	0.9986	1.029
29	1.24	29.15	34.17	1.197	1.236	1.128	10.22	10.63	1.111	1.144
30	1.386	32.42	38.04	1.332	1.376	1.255	10.97	11.39	1.23	1.268
31	1.544	35.92	42.18	1.476	1.525	1.39	11.75	12.19	1.358	1.399
32	1.712	39.67	46.62	1.63	1.684	1.534	12.56	13.01	1.494	1.539
33	1.893	43.67	51.36	1.795	1.855	1.688	13.39	13.86	1.639	1.687
34	2.086	47.93	56.41	1.971	2.036	1.851	14.26	14.75	1.791	1.845
35	2.292	52.46	61.78	2.158	2.229	2.023	15.16	15.66	1.953	2.011
36	2.511	57.27	67.48	2.356	2.434	2.206	16.09	16.6	2.124	2.187
37	2.743	62.36	73.52	2.566	2.651	2.398	17.05	17.57	2.304	2.372
38	2.99	67.75	79.91	2.788	2.88	2.601	18.04	18.58	2.493	2.566
39	3.25	73.44	86.66	3.023	3.123	2.814	19.05	19.61	2.692	2.771
40	3.526	79.44	93.77	3.27	3.378	3.038	20.1	20.68	2.901	2.985
41	3.816	85.77	101.3	3.531	3.647	3.273	21.19	21.77	3.12	3.21
42	4.123	92.42	109.2	3.805	3.931	3.519	22.3	22.9	3.349	3.445
43	4.445	99.4	117.4	4.093	4.228	3.776	23.44	24.06	3.588	3.69
44	4.783	106.7	126.1	4.395	4.54	4.045	24.61	25.25	3.838	3.947
45	5.139	114.4	135.2	4.712	4.867	4.325	25.82	26.47	4.098	4.214
46	5.511	122.5	144.8	5.044	5.21	4.617	27.05	27.72	4.369	4.492
47	5.901	130.9	154.8	5.391	5.568	4.921	28.32	29	4.651	4.782
48	6.309	139.7	165.2	5.753	5.942	5.238	29.61	30.31	4.945	5.083
49	6.736	148.9	176.1	6.131	6.333	5.566	30.94	31.65	5.249	5.395
50	7.181	158.4	187.5	6.526	6.741	5.907	32.3	33.02	5.566	5.72
51	7.646	168.4	199.3	6.937	7.165	6.261	33.69	34.43	5.894	6.056
52	8.13	178.8	211.6	7.365	7.607	6.628	35.11	35.86	6.233	6.404
53	8.635	189.6	224.5	7.81	8.067	7.007	36.56	37.32	6.585	6.765
54	9.159	200.9	237.8	8.273	8.545	7.4	38.04	38.82	6.949	7.138
55	9.705	212.6	251.6	8.754	9.042	7.806	39.55	40.35	7.325	7.523
56	10.27	224.7	266	9.253	9.557	8.226	41.09	41.9	7.713	7.921
57	10.86	237.3	280.9	9.77	10.09	8.659	42.67	43.49	8.114	8.332
58	11.47	250.3	296.4	10.31	10.65	9.106	44.27	45.11	8.528	8.756
59	12.1	263.8	312.5	10.86	11.22	9.566	45.91	46.76	8.954	9.193
60	12.76	277.8	329.1	11.44	11.82	10.04	47.57	48.44	9.394	9.643
61	13.44	292.3	346.2	12.03	12.43	10.53	49.27	50.15	9.847	10.11
62	14.14	307.3	364	12.65	13.07	11.03	51	51.89	10.31	10.58
63	14.87	322.8	382.4	13.29	13.72	11.55	52.76	53.67	10.79	11.07
64	15.62	338.8	401.3	13.94	14.4	12.08	54.55	55.47	11.28	11.58
65	16.4	355.3	420.9	14.62	15.1	12.63	56.37	57.3	11.79	12.1
66	17.2	372.3	441.2	15.32	15.83	13.19	58.22	59.17	12.31	12.63
67	18.03	389.9	462	16.05	16.58	13.77	60.1	61.06	12.84	13.18
68	18.88	408	483.5	16.79	17.34	14.36	62.01	62.99	13.39	13.74
69	19.76	426.7	505.7	17.56	18.14	14.97	63.95	64.94	13.96	14.31
70	20.67	446	528.5	18.35	18.95	15.59	65.93	66.93	14.53	14.9
71	21.6	465.8	552.1	19.17	19.8	16.23	67.93	68.95	15.12	15.51
72	22.56	486.2	576.3	20	20.66	16.88	69.96	70.99	15.73	16.12
73	23.55	507.2	601.2	20.87	21.55	17.55	72.03	73.07	16.35	16.76
74	24.57	528.8	626.8	21.75	22.47	18.23	74.13	75.18	16.98	17.41
75	25.62	551	653.1	22.66	23.41	18.93	76.25	77.32	17.63	18.07
76	26.7	573.8	680.2	23.6	24.38	19.65	78.41	79.49	18.3	18.75
77	27.81	597.2	708	24.56	25.37	20.38	80.6	81.69	18.98	19.44
78	28.94	621.3	736.5	25.55	26.39	21.13	82.82	83.92	19.67	20.15
79	30.11	646	765.8	26.56	27.44	21.9	85.07	86.19	20.38	20.88
80	31.31	671.4	795.9	27.6	28.51	22.68	87.35	88.48	21.1	21.62

Table S3. **Lifetimes of Rydberg states in ^{85}Rb.** Lifetimes calculated with *AlkCalc* [37] for principal quantum numbers $20 \leq n \leq 80$. Values are in microseconds (µs) and given to four significant digits. 'rad' denotes radiative ($T = 0\,\mathrm{K}$) lifetimes, while 'bbr' denotes room-temperature ($T = 300\,\mathrm{K}$) lifetimes, which are reduced by black-body-radiation-induced transitions.

n	$S_{\frac{1}{2}}$(rad)	$P_{\frac{1}{2}}$(rad)	$P_{\frac{3}{2}}$(rad)	$D_{\frac{3}{2}}$(rad)	$D_{\frac{5}{2}}$(rad)	$S_{\frac{1}{2}}$(bbr)	$P_{\frac{1}{2}}$(bbr)	$P_{\frac{3}{2}}$(bbr)	$D_{\frac{3}{2}}$(bbr)	$D_{\frac{5}{2}}$(bbr)
20	6.104	14.12	13.16	7.49	7.389	4.633	8.827	8.467	5.944	5.891
21	7.252	16.66	15.53	8.716	8.599	5.397	10.1	9.696	6.809	6.75
22	8.537	19.49	18.17	10.07	9.936	6.231	11.46	11.02	7.747	7.68
23	9.964	22.63	21.1	11.56	11.41	7.138	12.91	12.43	8.758	8.685
24	11.54	26.09	24.32	13.2	13.02	8.119	14.47	13.95	9.846	9.765
25	13.28	29.88	27.87	14.98	14.78	9.175	16.11	15.55	11.01	10.92
26	15.19	34.03	31.74	16.92	16.69	10.31	17.86	17.25	12.25	12.16
27	17.27	38.55	35.95	19.02	18.76	11.52	19.7	19.05	13.58	13.47
28	19.53	43.45	40.52	21.29	21	12.81	21.64	20.94	14.98	14.86
29	21.98	48.76	45.47	23.74	23.41	14.18	23.68	22.93	16.46	16.34
30	24.62	54.48	50.8	26.36	26	15.63	25.81	25.02	18.03	17.9
31	27.48	60.63	56.54	29.18	28.78	17.16	28.04	27.2	19.68	19.54
32	30.54	67.23	62.7	32.19	31.75	18.78	30.37	29.48	21.42	21.27
33	33.83	74.29	69.28	35.4	34.92	20.48	32.8	31.86	23.24	23.08
34	37.34	81.84	76.32	38.82	38.29	22.27	35.33	34.34	25.15	24.98
35	41.09	89.88	83.82	42.46	41.88	24.14	37.96	36.92	27.15	26.96
36	45.08	98.43	91.79	46.32	45.68	26.09	40.69	39.59	29.23	29.04
37	49.32	107.5	100.3	50.4	49.71	28.14	43.51	42.37	31.41	31.2
38	53.82	117.1	109.2	54.72	53.97	30.27	46.44	45.24	33.67	33.45
39	58.58	127.3	118.7	59.28	58.46	32.49	49.46	48.21	36.02	35.79
40	63.62	138.1	128.7	64.09	63.21	34.8	52.59	51.28	38.46	38.22
41	68.94	149.4	139.3	69.15	68.2	37.2	55.81	54.45	41	40.74
42	74.55	161.3	150.5	74.48	73.45	39.69	59.13	57.72	43.63	43.36
43	80.45	173.9	162.2	80.07	78.96	42.27	62.56	61.09	46.34	46.06
44	86.66	187.1	174.5	85.93	84.74	44.94	66.08	64.55	49.16	48.86
45	93.18	201	187.4	92.08	90.81	47.7	69.7	68.12	52.06	51.76
46	100	215.5	201	98.51	97.15	50.55	73.43	71.79	55.06	54.74
47	107.2	230.7	215.2	105.2	103.8	53.5	77.25	75.55	58.15	57.82
48	114.7	246.7	230	112.3	110.7	56.53	81.17	79.42	61.34	60.99
49	122.5	263.3	245.5	119.6	117.9	59.66	85.2	83.39	64.62	64.26
50	130.7	280.7	261.7	127.2	125.5	62.89	89.32	87.45	68	67.63
51	139.3	298.8	278.6	135.2	133.3	66.2	93.54	91.62	71.47	71.09
52	148.2	317.6	296.2	143.5	141.5	69.61	97.87	95.88	75.04	74.64
53	157.5	337.3	314.5	152.1	150	73.12	102.3	100.2	78.7	78.29
54	167.1	357.8	333.6	161.1	158.9	76.72	106.8	104.7	82.46	82.04
55	177.2	379	353.4	170.4	168	80.41	111.4	109.3	86.32	85.88
56	187.6	401.1	374	180.1	177.6	84.2	116.2	113.9	90.28	89.83
57	198.5	424.1	395.4	190.1	187.5	88.09	121	118.7	94.33	93.86
58	209.7	447.9	417.6	200.5	197.7	92.07	125.9	123.6	98.48	98
59	221.4	472.5	440.6	211.3	208.3	96.14	130.9	128.5	102.7	102.2
60	233.5	498.1	464.4	222.4	219.3	100.3	136.1	133.6	107.1	106.6
61	246.1	524.5	489.1	233.9	230.7	104.6	141.3	138.8	111.5	111
62	259.1	551.9	514.6	245.9	242.4	108.9	146.6	144	116.1	115.5
63	272.5	580.3	541	258.2	254.6	113.4	152.1	149.4	120.7	120.2
64	286.4	609.5	568.3	270.9	267.1	118	157.6	154.9	125.5	124.9
65	300.7	639.8	596.5	284.1	280.1	122.6	163.2	160.4	130.3	129.7
66	315.5	671	625.7	297.6	293.5	127.4	169	166.1	135.2	134.6
67	330.8	703.3	655.7	311.6	307.2	132.2	174.8	171.9	140.3	139.7
68	346.6	736.5	686.7	326	321.5	137.2	180.7	177.8	145.4	144.8
69	362.9	770.8	718.7	340.9	336.1	142.2	186.8	183.7	150.7	150
70	379.7	806.1	751.6	356.2	351.2	147.4	192.9	189.8	156	155.3
71	397	842.5	785.6	371.9	366.7	152.6	199.1	196	161.4	160.8
72	414.8	880	820.5	388.1	382.7	157.9	205.5	202.2	167	166.3
73	433.1	918.6	856.5	404.8	399.1	163.4	211.9	208.6	172.6	171.9
74	452	958.3	893.5	422	416	168.9	218.4	215.1	178.4	177.6
75	471.4	999.1	931.5	439.6	433.4	174.5	225.1	221.6	184.2	183.5
76	491.4	1041	970.6	457.7	451.3	180.3	231.8	228.3	190.1	189.4
77	511.9	1084	1011	476.3	469.6	186.1	238.6	235.1	196.2	195.4
78	533	1128	1052	495.4	488.4	192	245.6	242	202.3	201.6
79	554.6	1174	1095	515	507.8	198	252.6	248.9	208.6	207.8
80	576.8	1221	1138	535.1	527.6	204.2	259.8	256	214.9	214.1

and

$$\Delta_{\mathrm{bbr}} = \max_{20\leq n\leq 80} \frac{|\tau_{\mathrm{bbr}}^{\mathrm{model}}(n) - \tau_{\mathrm{bbr}}(n)|}{\tau_{\mathrm{bbr}}(n)}\,, \tag{S4}$$

for the parameters τ_s, δ, A, B, C, and D returned by the fit and listed in Tab. S4. These formulas give the 'worst-case' relative error when the formulas (S1) and (S2) are compared to the numerically obtained lifetimes τ_{rad} and τ_{bbr} given in Tabs. S1, S2, and S3.

Table S4. **Results for fitting parameters.** Fitting parameters for calculating Rydberg-state lifetimes with formulas (S1) and (S2). Δ_{rad} and Δ_{bbr} are the maximal relative errors for the radiative lifetimes ($T = 0\,\mathrm{K}$) and the lifetimes reduced by black-body radiation at room temperature ($T = 300\,\mathrm{K}$), respectively. Please see Eqs. (S3) and (S4) for their definition. The quantum defects, $\delta_{l,j}$, are taken from Refs. [8, 56–58] and are *not* determined by the fit. For $^{88}\mathrm{Sr}^+$ and $^{40}\mathrm{Ca}^+$ we use the same quantum defects for both $j = |l - 1/2|$ and $j = l + 1/2$. This is justified by the quality of the fits (see results for Δ_{rad} and Δ_{bbr}).

		$\delta_{l,j}$	τ_s[ns]	δ	A[ns^{-1}]	B	C	D	Δ_{rad}[‰]	Δ_{bbr}[‰]
$^{40}\mathrm{Ca}^+$	$\mathrm{S}_{\frac{1}{2}}$	1.802995	0.0643439	2.99664	1.71505	0.635144	2.17461	4.10589	11	2
	$\mathrm{P}_{\frac{1}{2}}$	1.4369	1.38617	2.97545	1.07581	0.36716	2.01395	4.00075	25	3
	$\mathrm{P}_{\frac{3}{2}}$	1.4369	1.47706	2.97644	1.00293	0.338701	1.99146	3.97992	21	3
	$\mathrm{D}_{\frac{3}{2}}$	0.626888	0.071956	3.00077	0.223293	0.0627589	1.43837	3.43424	2	(< 1)
	$\mathrm{D}_{\frac{5}{2}}$	0.626888	0.0728951	3.00083	0.215423	0.0601441	1.42447	3.42138	2	(< 1)
$^{88}\mathrm{Sr}^+$	$\mathrm{S}_{\frac{1}{2}}$	2.707	0.0686609	2.9971	1.65612	0.595327	2.1807	4.11765	11	3
	$\mathrm{P}_{\frac{1}{2}}$	2.31	1.73319	2.95583	1.16722	0.429748	2.03218	4.00522	59	2
	$\mathrm{P}_{\frac{3}{2}}$	2.31	2.01096	2.96084	0.878713	0.308999	1.937	3.91793	34	4
	$\mathrm{D}_{\frac{3}{2}}$	1.456	0.057733	2.99692	0.916547	0.344931	1.90863	3.84306	7	2
	$\mathrm{D}_{\frac{5}{2}}$	1.456	0.0596584	2.99682	0.854725	0.32005	1.88614	3.82101	7	2
$^{85}\mathrm{Rb}$	$\mathrm{S}_{\frac{1}{2}}$	3.1311804	1.26667	3.0006	0.0371408	0.0422265	1.62668	3.61202	2	1
	$\mathrm{P}_{\frac{1}{2}}$	2.6548849	2.70159	2.99449	0.0333433	0.0414708	1.45403	3.42116	17	2
	$\mathrm{P}_{\frac{3}{2}}$	2.6416737	2.51389	2.99482	0.0323853	0.0402913	1.43772	3.40454	15	1
	$\mathrm{D}_{\frac{3}{2}}$	1.34809171	1.15449	2.98878	0.213663	0.312492	2.06666	4.01305	32	3
	$\mathrm{D}_{\frac{5}{2}}$	1.34646572	1.13923	2.98858	0.215494	0.317436	2.06616	4.01158	32	3